Ceramics International **23** (1997) 61–68
© 1996 Elsevier Science Limited and Techna S.r.l.
Printed in Great Britain. All rights reserved
0272-8842(95)00141-7
0272-8842/97 $17.00 + .00

SHS Powders for Thermal Spray Applications

Cecilia Bartuli,[a] Ronald W. Smith[b] & Emil Shtessel[c]

[a]Dipartimento di Ingegneria Chimica dei Materiali, Materie Prime e Metallurgia, Università "La Sapienza", Via Eudossiana 18, 00184, Rome, Italy
[b]Centre for Plasma Processing of Materials, Department of Materials Engineering, Drexel University, 32nd and Chestnut Streets, Philadelphia, PA, USA
[c]Exotherm Corporation, 1035 Line Street, Camden, NJ, USA

(Received 29 June 1995; accepted 4 October 1995)

Abstract: Self-propagating high temperature synthesis (SHS) is defined as a combustion process in which reagents, when ignited, spontaneously transform, to complete conversion, into products, due to the exothermic heat of reaction. This process has been recently recognised as a very promising technique for materials processing: ceramics, intermetallics and cermets with good physico-chemical properties have been produced at low costs. The use of SHS products for thermal spray applications represents a natural evolution of the technique. Demanded characteristics for thermal spray feedstock powders can be very different, depending on the spraying process, the operating conditions, the desired properties of the final coating, etc. However, technical requirements can also be extremely rigid and detailed. As a consequence, the production process must be reliable and flexible, while remaining possibly inexpensive. SHS is investigated as a promising candidate technique for the production of different powders to be used for thermal spray coatings with different applications: metallic mixtures are considered, as well as ceramic and composite powders. The chemical and morphological features of different SHS powders are described, and their technical characteristics of flowability and sprayability are outlined. Wear performance and hardness tests results for some of the coatings obtained by both air and vacuum plasma spraying of SHS powders are also reported. © 1996 Elsevier Science Limited and Techna S.r.l.

1 INTRODUCTION

Historically, work on self-sustaining reactions developed from the study of conventional combustion processes and pyrochemical technologies.[1] The SHS technique evolved, however, in the late 1960s with the fundamental contribution of Soviet researchers (see Ref. 2 for a complete outline of the Soviet work on SHS), showing its enormous potential in the field of materials processing.

A wide variety of materials have been produced ever since by SHS, including metals, carbides, nitrides, borides, silicides, intermetallics and composite materials.[3,4] Many of these materials possess unique sinterability characteristics which cannot be obtained using other synthesis techniques.[5]

The SHS method offers several advantages. Purity has been sometimes reported[6,7] as a major quality of combustion synthesis, guaranteed by the very high temperatures approached during the process, which allow volatile compounds present as impurities to evaporate. It can be difficult to exert full control on the degree of completion of the synthesis reaction.

Moreover, the energy necessary for the synthesis of refractory compounds is self-generated by the heat of reaction, thus avoiding the exigency to maintain high temperatures for long times in furnaces. Also, the equipment used for the SHS process is usually very simple, thus dramatically reducing the initial costs with respect to conventional methods.

Finally, in the case of particulate-reinforced composites, SHS offers the advantage of forming nascent/coherent interfaces between the matrix and the products of the synthesis reactions. Any volume fraction of reinforcement is virtually achievable.

In this article the possibility is investigated of using powders of different compositions obtained by combustion synthesis as starting materials for thermal spray processes.

These powders are characterized from the physico-chemical, morphological and technical points of view, in order to verify whether they meet the fundamental requirements of thermal spray feedstock materials: can stoichiometry and phase composition of the powders be easily controlled? Are morphology and size distribution compatible with flowability and sprayability exigencies?

Coatings obtained by spraying SHS powders using both air and vacuum plasma spray are also tested. Hardness and wear resistance tests results are compared, when possible, with those obtained for coatings of the same compositions sprayed by conventional powders.

2 THE SHS PROCESS

Self-propagating high temperature synthesis is a particular combustion process in which an exothermic, self-sustaining chemical reaction proceeds layer by layer into the reaction volume, gradually transforming the reactant powder mixture into the desired products.

Any physical phase can be involved in the combustion process: however, at least one of the reactants should form a liquid or vapour phase, in order to increase the diffusion rate towards the reaction front and, consequently, the global velocity of the whole combustion process.[7] Highest propagation velocities are achieved, according to Ref. 8 when a liquid component spreads in the compact constituted by the other, solid reactant.

One of the main parameters used for describing an SHS process is the adiabatic temperature (T_{ad}), defined as "the maximum temperature to which the products are raised under adiabatic conditions as a consequence of the evolution of heat during the chemical reaction".[9] The kinetics of the combustion reaction, the structure and the velocity of the combustion wave and the mechanisms of the single reactions taking place during an SHS process are direct or indirect functions of the adiabatic temperature and of the (melting point/adiabatic temperature) ratio for the single reactants. T_{ad} values range, for different processes, from about 1200 to 6000 K.

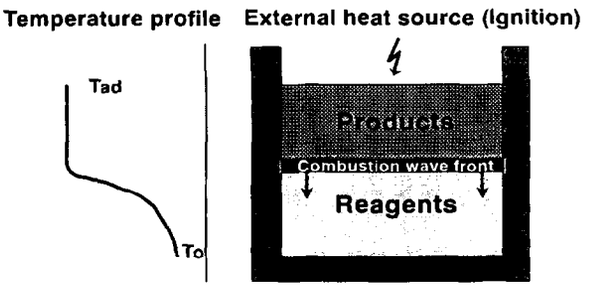

Fig. 1. Schematic representation of an SHS process: the temperature profile in the reaction volume is indicated on the left side.

Figure 1 shows a schematic representation of an SHS reaction. After ignition with an external source (electric arc, laser, tungsten heating coil, oxyacetylene torch, or other), reactants and products are separated by a combustion wave front, moving through the reaction volume with a constant velocity ranging from about 0·1 to 10 $cm \cdot s^{-1}$. Spatial distribution of T_{ad} in the system is also qualitatively illustrated.

3 THERMAL SPRAY FEEDSTOCK REQUIREMENTS

Powders for thermal spray applications generally need to satisfy the following requirements.[10]

- *Size and morphology*: morphology can affect parameters such as powders feed rate, effective dwell time in the plasma, packing in the powder feeder. Coarse and rounded particles are best for good flowability through the torch. A narrow size distribution would be recommended. Repeatability and effectiveness of the classification process should be guaranteed.
- *Chemical control*: depending on the manufacturing method, metallic powders may either be coated by an oxide layer, or contain small amounts of oxygen in solution inside the particle. This feature can affect some of the coating properties, such as hardness, wear resistance, cohesion/adhesion, elastic modulus, etc. In the case of composite coatings, the metal/metal or ceramic/metal intimate mixing can be better achieved by using composite powders; the powder manufacturing process should guarantee optimal metal/metal or ceramic/metal contacts.
- *Costs*: costs obviously play a first rate role in the evaluation of a manufacturing process. A complete analysis should also take into account the need for post-treatments (agglomeration, sintering, plasma densification...) and the ease of classification.

Table 1. SHS parameters

Products	Combustion temperature (°C)	Combustion rate (cm/s)	Precursors size
$MoSi_2$	1590	0·38	‹325 mesh Mo+Si
NiCr	1450	0·18	‹325 mesh Ni+Cr+Ti
+40%TiC			‹1 μm carbon black
NiCr	1830	0·24	‹325 mesh Ni+Cr+Ti
+60%TiC			‹1 μm carbon black

- *High productivity and process reliability and flexibility* are necessary premises for the success of an industrial-rate manufacturing process.

4 EXPERIMENTAL

SHS powders of the following compositions:

1. $MoSi_2$
2. 40% vol (80% vol. Ni + 20% vol. Cr) + 60% vol. TiC
3. 60% vol (80% vol. Ni + 20% vol. Cr) + 40% vol. TiC

were produced by reacting elemental blends, prepressed in 8 cm pellets, in a reactor with thermally insulated walls, in argon atmosphere. Initial density of the pellets was 50% of the theoretical density. Ignition was carried out by means of a tungsten filament. Small quantities (less than 1% wt) of proprietary additives were also added to the initial mixture in order to increase the velocity of propagation of the reaction front, and to modify the wettability of the mixture in the case of melting of one of the initial components during the reaction. The synthesis chemical reactions are indicated as follows:

1. $Mo + 2\,Si \rightarrow MoSi_2$,
2, 3. $Ti + C \rightarrow TiC$

All powders were obtained from compacted elemental reactants of different initial size. Combustion temperature, combustion rate and particle size of the precursors are summarized in Table 1 for the three SHS powders. Products of the synthesis (about 60% dense) were milled and screened to the final nominal size distribution indicated in Table 2. $MoSi_2$ (< 25 μm, > 5 μm) and NiCr40%TiC (< 325 mesh, > 15 μm) powders, produced by conventional agglomeration and sintering (A & S) and plasma densification (P.D.), respectively, were also characterized for comparison. Air and vacuum plasma spray coatings were deposited on to grit blasted 4140 stainless steel coupons (25 × 75 × 1·5 mm). 4140 steel discs (70 mm Ø × 2 mm) were also coated for wear resistance evaluation. Spray parameters are summarized in Table 2.

Samples from the powders and/or polished sections of the plasma sprayed coatings (polishing procedure: 300 mesh SiC grinding paper and TBW diamond impregnated discs) were characterized by scanning electron microscopy (Philips SEM 505, 20–25 kV accelerating tension).

X-ray diffraction analyses (Siemens D500 diffractometer, Cu kα Ni filtered radiation, 2θ range 20–90°, scanning step 0·05°, scanning time 1 s) of the powders and of whole samples of the coatings were carried out for phase identification, and to investigate any possible compositional change occurred during plasma spray.

Size distribution of the powders was analysed by means of laser light scattering (Malvern Mastersizer) in a liquid disperdant (distilled water). The water containing the powder sample was stirred during the measurement, and ultrasonic treatment was sometimes applied (about 1 min) in order to dissolve clusters or physical aggregates of particles possibly formed due to their irregular morphology. For the final calculation a round shape of all particles was assumed.

Table 2. Plasma spray parameters (APS and VPS)

Material	Nominal size	Atmosphere (Torr)	Plasma Gas 1/ (scfh)	Plasma Gas 2/ (scfh)	Carrier gas/ (scfh)	Spray distance (cm)	Arc current (A)	Arc voltage (V)	Coating thickness (mm)
$MoSi_2$ (SHS)	‹325 mesh	VPS 200	Ar/125	H_2/17	Ar/18	11	1100	47	0·375
$MoSi_2$ (A&S)	‹25 μm, ›5 μm	VPS 200	Ar/125	H_2/17	Ar/18	11	1100	47	0·35
NiCr+60% TiC (SHS)	‹325 mesh	VPS 200	Ar/140	He/60	Ar/18	17·5	1000	37	0·25
NiCr+60% TiC (SHS)	‹325 mesh	APS 760	Ar/125	He/60	Ar/27	9	1000	38	0·35
NiCr+40% TiC (SHS)	‹270 mesh	VPS 200	Ar/140	He/70	Ar/18	17·5	1100	47	0·35
NiCr+40% TiC (P.D.)	‹325 mesh ›15 μm	VPS 200	Ar/140	He/60	Ar/18	17·5	1100	50	0·275

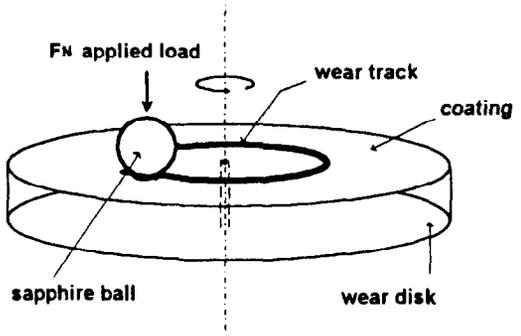

Fig. 2. Schematic representation of the wear testing apparatus.

Coatings were finally characterized on the basis of their microhardness and wear resistance. For microhardness measurements on polished sections of the coatings, a LECO M400 Vickers micro-indentator was used, with a load of 300 g applied for 10 s.

Unlubricated pin-on-disc wear testing was performed in dry air on ground and polished plasma sprayed coatings on discs (ASTM G99-90). The sliding counterbody was an Al_2O_3 (sapphire) ball, 10 mm Ø. A normal load of 20 N was generally applied, and a coating/counterbody relative velocity of 0·44 m/s was set. Wear tracks after 10,000 cycles were observed and areas were measured by a steel stylus profilometer. Figure 2 shows a schematic representation of the test setting.

5 RESULTS AND DISCUSSION

The powders

Size distributions of the SHS $MoSi_2$, NiCr + 40%TiC and NiCr + 60%TiC powders, as obtained by laser light scattering, are illustrated in Fig. 3 (a), (b) and (c). A cumulative curve and a histogram are plotted for each sample.

As it can be observed, $MoSi_2$ powder (Fig. 3(a)) exhibits a narrow size distribution around the mean value (35 μm). About 75% of the particles fall in the 20–60 μm range. About 75% of the particles are under 45 μm, specified as the maximum size. No ultrasound treatment was necessary in this case to break down particle aggregates.

SHS NiCr + TiC powders distributions are wider and almost bimodal. In particular, in the case of the NiCr40%TiC powder (see Fig. 3(b)), 65% of the particles are between 20 and 80 μm, distributed around the first peak, at about 50 μm. 20% of the particles, however, fall in the 0·5–10 μm, more or less distributed around the second peak, at about 2 μm. NiCr60%TiC (Fig. 3(c)) shows a similar behaviour. Ultrasounds were applied for 1 min for better dispersion. It should be noted that the 'tail'

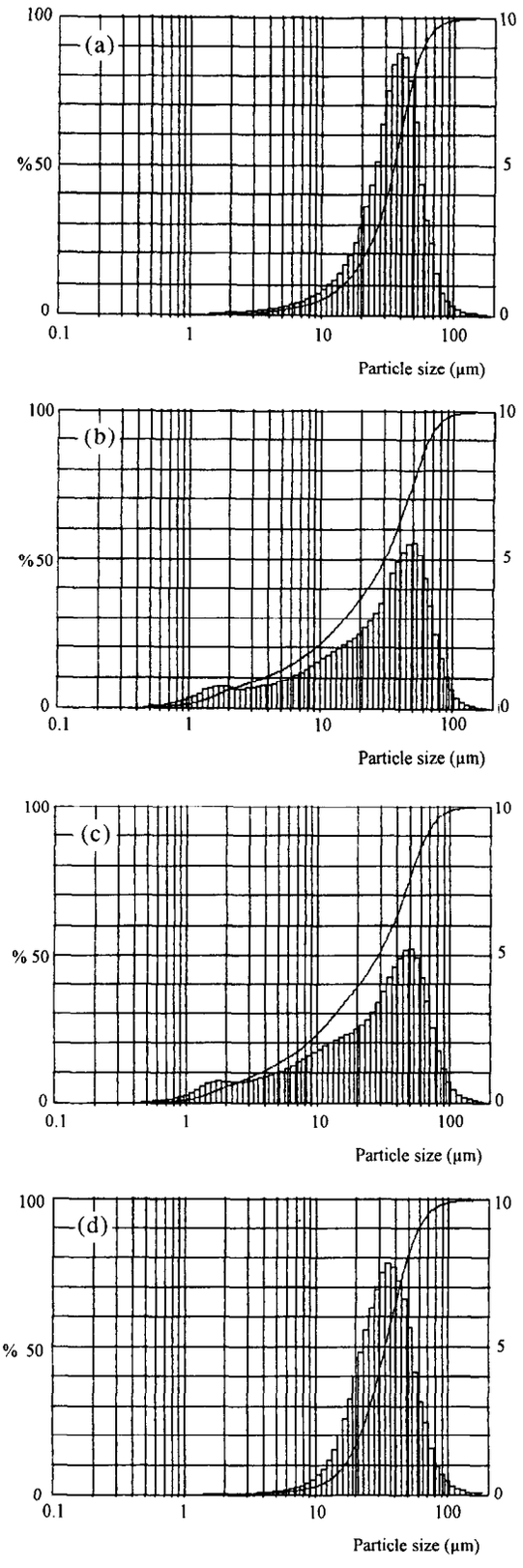

Fig. 3. Size distribution (histogram and cumulative curve) of the powders as obtained by laser light scattering: (a) SHS $MoSi_2$; (b) SHS NiCr40%TiC; (c) SHS NiCr60%TiC; (d) P.D. NiCr40%TiC.

of the gaussian distribution of these powders towards the low sizes cannot be cut down simply by mechanical sieving, because of the immediate clogging of the sieve holes caused by the irregular fine particles. Air classification would be recom-

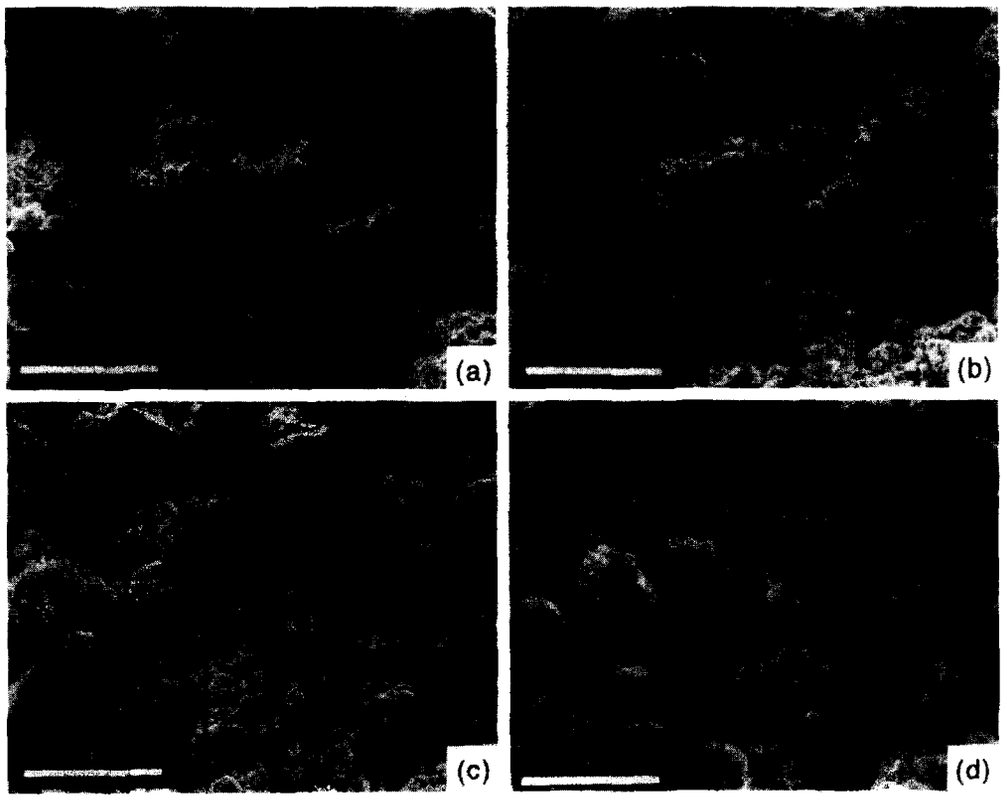

Fig. 4. SEM micrographs of the powders: (a) SHS $MoSi_2$; (b) SHS NiCr40%TiC; (c) SHS NiCr60%TiC; (d) plasma densified NiCr40%TiC.

mended. In Fig. 3(d) the narrower size distribution of the plasma densified powders with the same composition is reported for comparison.

SEM micrographs of SHS powders are illustrated in Fig. 4 (a, b and c). Results of the laser-sizing are confirmed, and more details on the irregular morphology are shown. $MoSi_2$ particles are rounded and characterized by a high inner porosity (Fig. 4(a)). NiCr + TiC powders are fragmented and angular-shaped (Fig. 4 (b) and (c)): fine particles (about 1–2 μm) are distributed on the surface and among larger grains (20–30 μm). The morphology of the P.D. NiCr + TiC powder is also shown for comparison (Fig. 4 (d)).

As expected on the basis of the results illustrated, the flowability of the SHS NiCr + TiC powder — i.e. its ability to flow through a given nozzle at given pressure (80 psi) and feeder rotation (3 rpm) — as compared to the P.D., is low. Experiments indicate a flowability of 23 g/min for the SHS powder against 38 g/min for the P.D. Again, air classification is probably the safest means to improve powders behaviour on their way to and through the nozzle.

X-ray diffraction patterns of SHS powders are illustrated in Fig. 5 ((a), (c) and (e)). $MoSi_2$ is present in the powders in the thermodynamically stable tetragonal phase, as expected from the very high synthesis temperature ($\gg$800°C). In the NiCr + TiC X-ray patterns, TiC and Ni are clearly identified. Peaks corresponding to Cr lines (even though partially covered by the overlapping Ni peaks) are very low, maybe indicating a chromium content in the matrix lower than the specified 20% vol.

The coatings

Figure 6 illustrates the microstructure of three coatings, obtained by vacuum plasma spray of SHS $MoSi_2$ (Fig. 6(a)), and by air plasma spray of SHS (Fig. 6(a)) and P.D. (Fig. 6(b)) NiCr + 40%TiC, respectively (SEM micrographs). The microstructure of the $MoSi_2$ coating is homogeneous; no phase separation is detectable; small pores are entangled among the layers formed by the different torch passes.

In the cross-sections of the NiCr + TiC coatings (Fig. 6 (b) and (c)) the dark areas represent TiC particles (as confirmed by EDS analyses), embedded in the metallic Ni–Cr matrix. Size, shape and distribution of the carbides are evidently very different in the two cases. SHS carbides are rounded and generally smaller, ranging from fractions of micron to 2–3 μm. The different size and distribution of the carbides in the matrix depend on the original distribution in the single drops impinging on the substrate. Nascent and coherent ceramic interfaces can guarantee better adhesion between the hard particles and the matrix. The angular-shaped carbides in the P.D. coating are shown in Fig. 6(b).

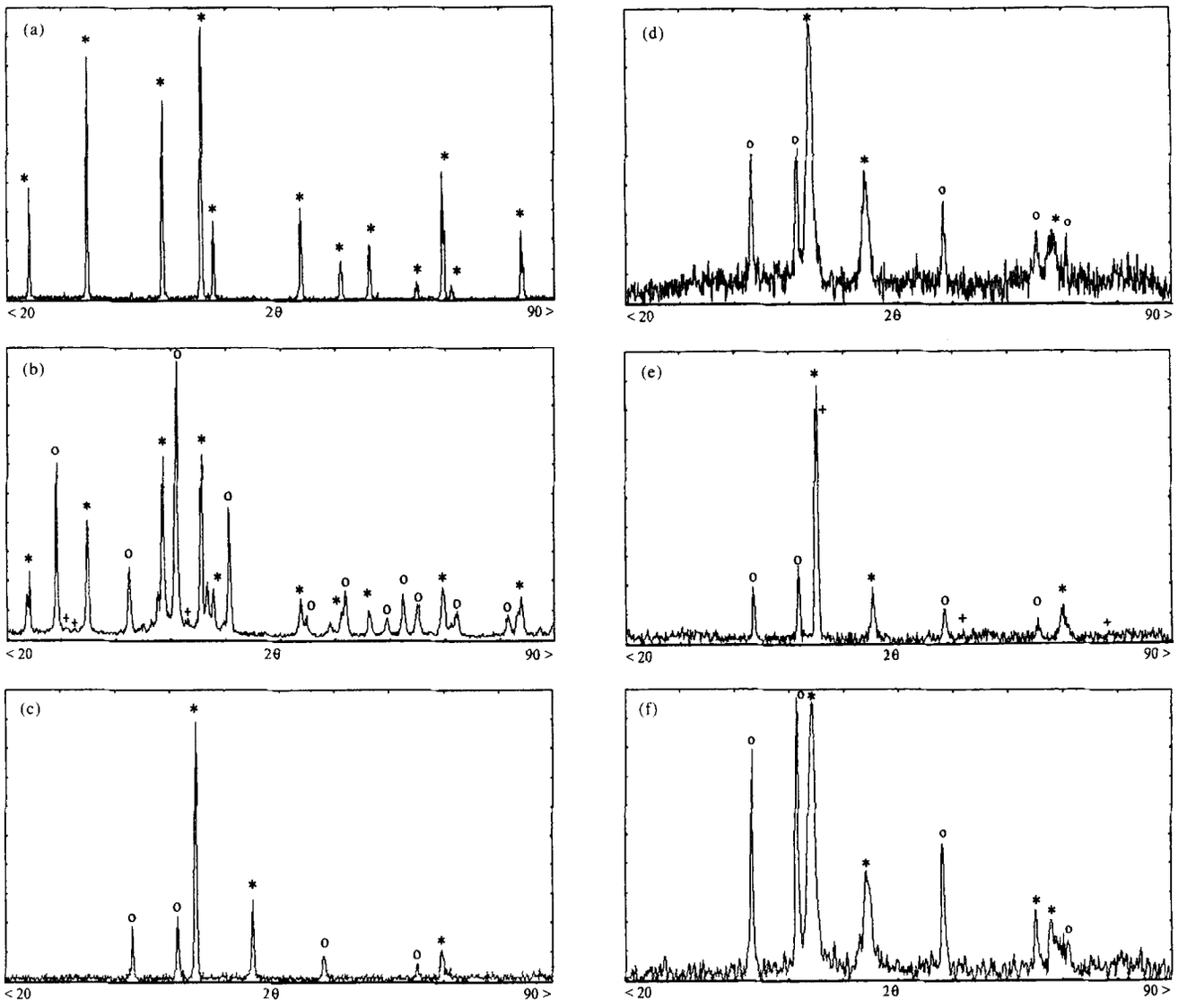

Fig. 5. X-ray diffraction patterns of SHS powders and coatings: (a) $MoSi_2$ powder (* = tetragonal $MoSi_2$); (b) $MoSi_2$ coating (* = tetragonal $MoSi_2$, ° = hexagonal $MoSi_2$, + = Mo_5Si_3); (c) NiCr40%TiC powder (* = TiC, ° = Ni); (d) NiCr40%TiC coating (* = Ni, ° = TiC); (e) NiCr60%TiC powder (*Ni, ° = TiC, + = Cr); (f) NiCr60%TiC coating (* = Ni, ° = TiC).

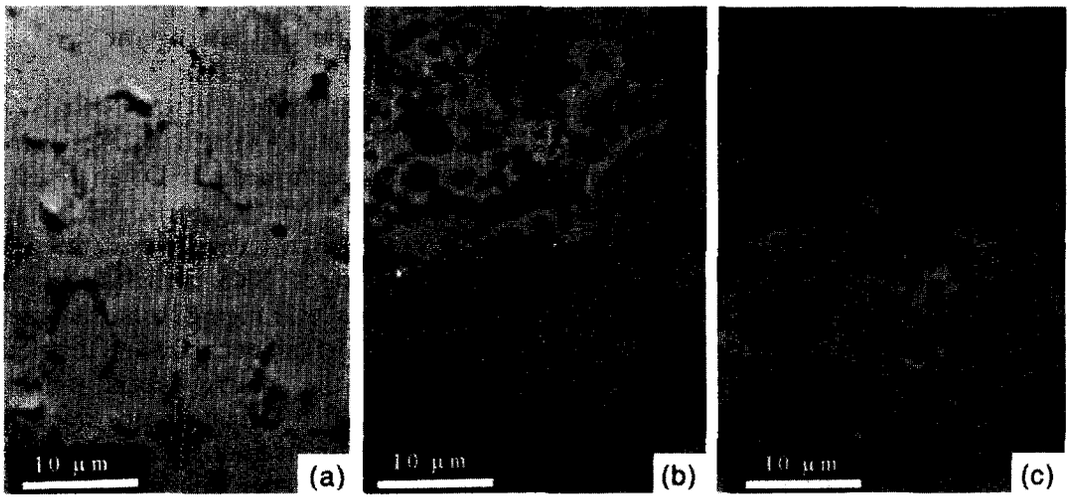

Fig. 6. Microstructure of plasma sprayed coatings (SEM): (a) SHS $MoSi_2$ (VPS); (b) SHS NiCr40%TiC (APS); (c) P.D. NiCr40%TiC (APS).

Table 3. Microhardness and wear tests results (normal load =20 N) for plasma sprayed coatings

Material	Powder production method	Spray process	VHN (kg/mm^2)	Coefficient of friction initial	Coefficient of friction final	Wear track area (μm^2)
$MoSi_2$	SHS	VPS	746	0·8 (*)	0·5 (*)	8820 (*)
$MoSi_2$	A.S.	VPS	898	—	—	—
NiCr40%TiC	SHS	APS	756	—	—	—
NiCr40%TiC	SHS	VPS	727	0·45(**)	0·55(**)	2764(**)
NiCr40%TiC	P.D.	APS	841	0·5	0·75	3861
NiCr40%TiC	P.D.	VPS	717	0·5	0·6	1330
NiCr60%TiC	SHS	APS	685	0·63	0·57	2131
NiCr60%TiC	SHS	VPS	326	0.55	0.44	350

(*)A normal load of 5 N was applied for the measurement.
(**)A normal load of 30 N was applied for the measurement.

X-ray diffraction patterns of the VPS coatings are reported in Fig. 5 ((b), (d) and (f)). A phase modification of the $MoSi_2$ is evident from the comparison with the pattern of the original powder (Fig. 5 (a)). The structure of the $MoSi_2$ in the plasma sprayed coating is equally distributed between the tetragonal and hexagonal phases. The presence of a relevant amount of the metastable hexagonal phase is a direct consequence of the rapid solidification of the remelted material.

No phase modification of the Ni–Cr + TiC powders during plasma spraying has been detected (see Fig. 5 (d) and (f)).

Microhardness and wear tests results for air and vacuum plasma sprayed coatings are illustrated in Table 3. $MoSi_2$ VPS coating from SHS powders exhibit a low hardness, as compared to the coating from A.S. powders. A poor wear performance of the SHS coating is also evidenced. Wear of the coating is extremely high, even if the normal load applied is only 5 N (coating failed to the substrate with higher loads). Friction coefficient is high, varying between 0·8 and 0·5.

SHS NiCr–TiC coatings, while exhibiting values of microhardness comparable or even lower than those of the corresponding P.D. coatings, are characterized by a much higher wear resistance in the conditions of the test. In particular, cross-sectional areas of the wear tracks of VPS SHS NiCr + 40%TiC coatings tested with a normal load of 20 N were so small to be practically unmeasurable: the value of 2764 μm^2, and the corresponding friction coefficients, reported in Table 3 for such coatings, were obtained in more severe testing conditions (normal load = 30 N). Preliminary results indicate that an increase in the TiC concentration from 40% to 60% vol. in the powders brought to a decrease of the hardness of the coating without sensible improvements in the wear resistance. A first explanation of the very satisfying wear behaviour of the SHS coatings can be found in the very good quality of the carbides–matrix interfaces, originated *in situ* during the synthesis process. The so-formed carbides are more coherent to the metallic matrix, and their pull-out during friction can therefore be limited. Further, the morphology of the TiC inclusions can play an important role in the wear mechanism: round-shaped carbides, such as those observed in the SHS coatings, can reduce — as compared to cutting, angular-shaped particles — the damage of the surface caused by the presence of a hard third body (the carbide itself) between the coating and the counterbody.

6 CONCLUSIONS

Concluding this preliminary work on the application of the self-propagating high temperature synthesis process to the production of powders for thermal spray, we try to give an answer to the main questions about general requirements of thermal spray feedstocks.

- The control of size and morphology remains a major shortcoming of the SHS technique, which necessarily involves a final step of mechanical crushing and grinding of the solid products. It is therefore difficult to guarantee the correct shape and size distribution of the grains and, as a consequence, to optimize powders flowability. A certain control could be exerted by operating on the density of the final 'sintered'
- The control of the chemical composition of the powders appears satisfying. Impurities or residual non-reacted compounds were not detected. Metal/ceramic interfaces are clean and seem to guarantee a very good quality of the matrix/reinforcement cohesion.

- Costs are certainly reduced with respect to other current production processes. No post-treatment is necessary, exception made, in some cases, for air classification.
- As far as the last point (high productivity and process reliability) is concerned, further investigations still need to be carried out on problems related to scale-up. As already mentioned, the flexibility of the process does not appear to represent a limitation of the SHS technique.

REFERENCES

1. MCCAULEY, J. W., *Ceram. Eng. Sci. Proc.*, **11**(9–10) (1990) 1137–9.
2. MERZHANOV, A. G., In *Combustion and Plasma Synthesis of High Temperature Materials*, ed. Z. A. Munir & J. B. Holt. VCH Publishers Inc., New York, 1990, pp. 1–53.
3. DUNMEAD, S. D., MUNIR, Z. A., HOLT, J. B. & KINGMAN, D. D., *J. Mater. Sci.*, **26** (1991) 2410–16.
4. MERZHANOV, A. G., In *Ceramics: Towards the 21st Century*, ed. N. Suga & A. Kato. The Ceramic Society of Japan, Tokyo, 1991, pp. 378–403.
5. PUSZYNSKI, J. A., MAJROWSKI, S. & HLAVACEK, V., *Ceram. Eng. Sci. Proc.*, **11**(9–10) (1990) 1182–9.
6. GREBE, H. A., ADVANI, A., THADHANI, N. N. & KOTTKE, T., *Metall. Trans.*, **23A** (1992) 2365–72.
7. CHOI, Y., MULLINS, M. E., WIJAYATILLEKE, K. & LEE, J. K., *Metall. Trans.*, **23A** (1992) 2387–92.
8. SHKIRO, V. M. & BOROVINSKAYA, I. P., *Fisika Gorenia i Vzriva*, **6** (1976) 945.
9. SUBRAHMANYAM, J. & VIJAYAKUMAR, M., *J. Mater. Sci.*, **27** (1992) 6249–73.
10. HERMANEK, F. J. & NICOLL, A. R., In *Thermal Spray: Advances in Coatings Technology*, ed. D. L. Houck. ASM International, Materials Park, OH, USA, 1988, pp. 337–44.